Random Walks for Quantum Mechanics

Laura da Palma Bárbara

Abstract In this paper, the first four energies of a particle in a 1D infinite potential well, a 2D infinite square well and a 2D infinite circular well were calculated using a Random Walk simulation with some accuracy. The simulations model the particle as a drunkard stepping in random directions along allowed axes, with the probability of them being arrested and ending their walk determined by a function of position and number of steps taken. This is taken to be an exponential function whose rate of arrest λ is directly related to the energy of the particle being modelled. The accuracy of the results is proven to be related to the arbitrarily chosen well length and the number of drunkards in the simulation. This paper also proves that, although this technique can become very computationally intensive when parameters are chosen to maximise result accuracy, it allows for the simulations to be extended to higher dimensions without deteriorating.

1 Introduction

As technology evolves, so does the scope of its applications in many fields, including computational physics. Physical problems that were once too computationally demanding can now be tackled with a large array of numerical analysis techniques. Random Walks (RWs) in particular have earned their place as a simple yet robust method that can be used to model processes, from genetic drift [1] to share prices [2], and easily lend themselves as a tool to solve perhaps one of the biggest hurdles physics has met – accurately computing the ground state energies of quantum systems.

In this work, the ground state energy of a 1D infinite potential well is estimated using RW simulations, where the "particle in a box" is treated as a drunkard stumbling their way through a street, at the ends of which are police officers waiting to arrest the drunkard. This model is then expanded upon, to obtain estimates of higher energies for the 1D well along with the 2D infinite square well and the 2D infinite circular well. Furthermore, the dependence of the estimate on the length of the well and the number of drunkards is investigated, and the limitations of the method are reported.

2 Theory and Assumptions

A simple 1-dimensional RW such as the one described in Appendix A can easily be used to model the behaviour of a particle in a 1D infinite potential well by introducing boundaries on the person's movement. A similar statement can be made for a 2D RW and a particle in a 2D infinite potential well.

2.1 1 Dimension

Suppose a drunkard sets off on a walk along a straight line. The drunkard is free to randomly step in either of the two allowed directions, both with equal probability. Their walk reaches its end as soon as they reach a position where a police officer arrests them.

Let $p(j,s+1)$ be the probability that the drunkard is at position j after taking $s+1$ steps, assuming they set off from $j=0$. This probability depends on $a(j)$, the probability of being arrested at position j, as well as the probability of the drunkard being in any of the adjacent points $j=\pm 1$ after s steps:

$$p(j,s+1) = \frac{1}{2}[1-a(j)][p(j-1,s) + p(j+1,s)] \tag{1}$$

Now let $a(j)$ be very small and s be very large, so that $p(j,s)$ can be considered a function of continuous variables j and s. Expanding the probabil-

ity terms using the Taylor series, Eq. (1) becomes a differential equation, which considering the ansatz:

$$p(j,s) = q(j)\exp(-\lambda s) \tag{2}$$

where λ is the rate of arrest and $q(j)$ an arbitrary spatial distribution, simplifies to:

$$-\frac{1}{2}\frac{d^2q(j)}{dj^2} + a(j)q(j) = \lambda q(j) \tag{3}$$

Eq. (3) has the same form as the 1D Schrödinger equation (SE), and this similarity can be used to find a relation between the drunkard's walk and the energy of a quantum system described by the SE.

For a 1D infinite potential well of length $2b$, the potential across all space is:

$$V(x) = \begin{cases} 0 & \text{if } -b < x < b \\ \infty & \text{otherwise} \end{cases}$$

Introducing a change of variables $x = b(j/J)$ so that $j = J$ corresponds to the drunkard reaching the edge of the well, the SE inside the well becomes:

$$-\frac{1}{2}\frac{d^2\psi(x)}{dj^2} = \frac{Emb^2}{\hbar^2 J^2}\psi(x) \tag{4}$$

Comparing Eq. (3) and Eq. (4), taking $a(j) = 0$ inside of the well, yields the relation:

$$E = \frac{\lambda\hbar^2 J^2}{mb^2} \tag{5}$$

Thus, using Eq. (2) to find λ for an arbitrarily chosen J, one can estimate the energy of the 1D infinite potential well, whose value for the n^{th} state is [3]:

$$E_n = \frac{\pi^2\hbar^2}{8mb^2}n^2 \tag{6}$$

2.2 2 Dimensions

In a 2D RW, the drunkard's position is given by two variables j_1 and j_2, which correspond to the x and y coordinates, respectively. The equivalent of the probability $p(j,s)$ in 2D is $p(j_1,j_2,s)$, given by the equation:

$$\begin{aligned} p(j_1,j_2,s+1) = \frac{1}{4}[1-a(j_1,j_2)][&p(j_1-1,j_2,s) \\ &+ p(j_1+1,j_2,s) + p(j_1,j_2-1,s) \\ &+ p(j_1,j_2+1,s)] \end{aligned} \tag{7}$$

Following a similar derivation as the one for the 1D well (please refer to Appendix C) yields an expression for the energies of a 2D well of side length $2b$:

$$E = \frac{2\lambda J^2\hbar^2}{mb^2} \tag{8}$$

The energy values for the 2D square well for the state with quantum numbers n_x, n_y are [4]:

$$E_{n_x,n_y} = \frac{\pi^2\hbar^2}{8mb^2}(n_x^2 + n_y^2) \tag{9}$$

The 2D circular well has energy values which depend on the k^{th} zero of the n^{th} Bessel function of the first kind, $\rho_{n,k}$ [5]:

$$E_{n,k} = \frac{\hbar^2}{2mb^2}\rho_{n,k}^2 \tag{10}$$

3 Method

Python 3 was used to implement a RW simulation in 1 and 2 dimensions, which can easily be extended to N higher dimensions by adding N spatial coordinates to the simulation.

The RW steps were generated using a Permuted Congruential Generator, which is discussed in further detail in Appendix B. For the 2D simulation, each time the drunkard took a step the PCG randomly chose a number (1 or 2) which dictated the axis of the step (x-axis or y-axis, respectively). It then chose a different number (-1 or 1) corresponding to the direction of the step along the axis (negative or positive, respectively. For the 1D walk, only the second choice took place, as there was only one possible axis on which to step.

The starting position of the walkers depended on the energy state being investigated in the simulation – they began their walk at a peak in the probability

function in the simulated well as this starting position was shown through experimentation to give the most accurate results.

Each drunkard's walk lasted until the boundary conditions for each of the simulations were violated. For the ground state energies, this meant until the drunkard reached the edge of the well whose length was chosen by the user. For higher energies, the walk ended once the drunkard reached a position corresponding to a node in wavefunction of a particle in the same well. This was repeated for an arbitrary number of drunkards, and the number of arrests that occurred at a certain amount of steps was obtained from a histogram of the number of steps each drunkard took until being arrested, as shown in Fig. 1a. The cumulative sum of the arrests was used to calculate the number of drunkards that made it to each amount of steps, as they are complementary, and finally the probability of 'surviving' up to n steps was obtained.

Two things to note in Fig. 1a are the fact that the histogram does not start at the origin and that its peak is not at the lowest value of s. The first feature is due to the fact that the drunkard must necessarily walk *at least* half the length of the well in order to reach the edge and be arrested. This is, of course, extremely rare, as it would require the drunkard to step in the same direction every single time. The low probability of being arrested after a small number of steps is what leads to the second feature of the histogram – as s increases so does the number of arrests, up to certain value after which the number of arrests starts to decrease exponentially. This offset peak leads to the calculated probability of survival not having a fully exponential decay with s, but instead having an inflection in the region of s values for which the peak occurs, which can be seen in Fig. 1b. This behaviour was accounted for by finding the value of s which had the maximum number of arrests and defining it as low cutoff point, essentially discarding any data for lower steps.

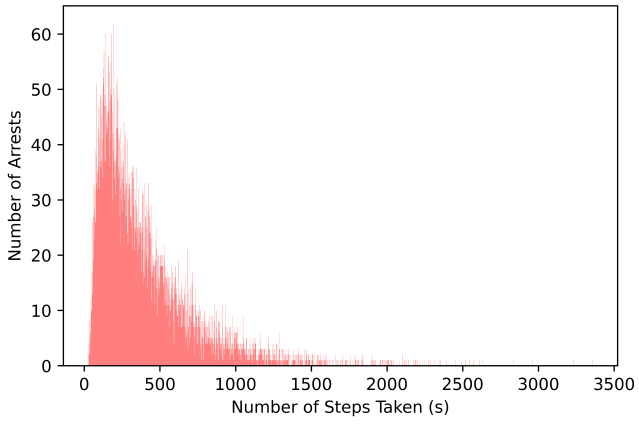

(a) caption

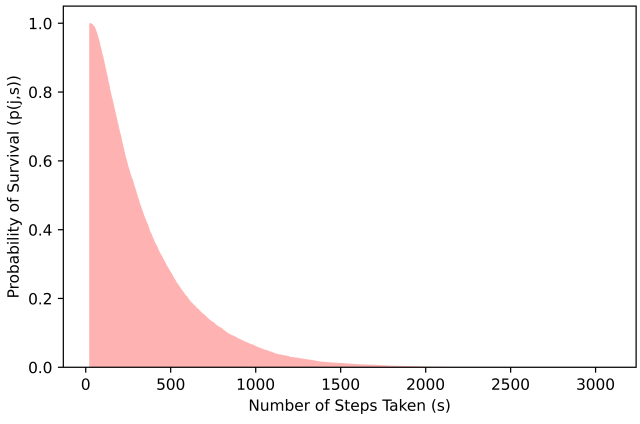

(b) caption

Figure 1: caption

Eq. (2) was then fitted to the probability of survival data using non-linear least squares curve fitting in order to find a value for λ.

The simulations were run 10 times for 10000 drunkards inside a 1D well, a 2D square well and a 2D circular well all with $J = 50$. The mean and standard deviation of the 10 simulations were calculated for each case.

A 1D simulation was carried out for 100 drunkards in wells with different values for J to investigate how the length of the well affected the results. Similarly, simulations with different amounts of drunkards in a well with $J = 8$ were carried out.

4 Results and Discussion

Six ground state simulations were run for 1D wells with arbitrary J values between 10 and 150, with 100 drunkards. Another three simulations were run for 1D wells of $J = 8$ with 1000, 10000 and 100000 drunkards each. The resulting λ values were then used to calculate λJ^2 for each simulation, which are shown in Fig. 2 along with the theoretical prediction $\pi^2/8$.

From Fig. 2a it can be verified that as J is increased the calculated λJ^2 approaches the theoret-

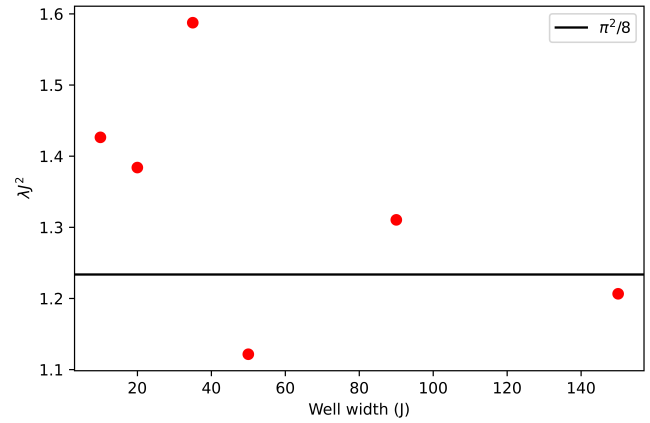

(a) caption

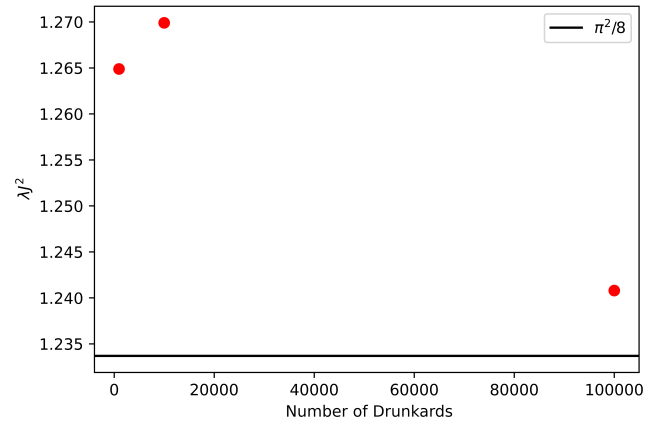

(b) caption

Figure 2: caption

ical prediction. This is due to the fact that a larger well means the drunkards will need to take a larger number of steps to reach the edge of the well. In Section 2, the number of steps s was assumed to be large in order for $p(j,s)$ to vary smoothly with j and s. Thus, a larger J value better satisfies this assumption and yields better estimates of the energies.

It can be seen in Fig. 2b that a larger amount of drunkards also improves the energy estimate. This is because a simulation with more drunkards effectively means a larger sample size and a smoother probability distribution $p(j,s)$ which, again, satisfies the assumption made in Section 2.

It must also be noted that the computing time was very long ($\sim$ 30 minutes) for the larger values of J and drunkard amounts. This means that it might be necessary to sacrifice some result accuracy if higher parameters are making the simulation too computationally intensive. In this project, all of the energy values were estimated using simulations of 10000 drunkards and wells with $J = 50$. These parameters were chosen taking into consideration both the accuracy of the results and the run time of the simulations in Python 3. Implementing the RW simulations in a faster language or running them in a faster system will allow for higher parameters to be used, which in turn yield more accurate results.

A 1D ground state simulation with the chosen parameters was run and the resulting data was fitted with an exponential curve of Eq. (2), as shown in Fig. 3. The best fitting parameters were found to be $q(j) = 1.28686$ and $\lambda = 0.00050$ with an R-squared value of 0.99944 which confirms the adopted ansatz. $\lambda J^2 = 1.25$ was calculated from the fit parameters and agrees with the theoretical value $\pi/8 = 1.23$ up to two significant figures. The parameter errors obtained from the covariance matrix of the fitted curve were negligible, therefore propagating it to the λJ^2 value was not useful. Instead, the final energy estimates and their error were obtained by repeating the simulations for a number of

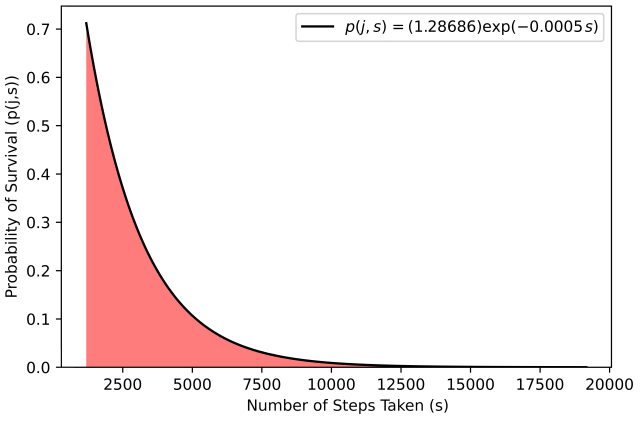

(a) caption

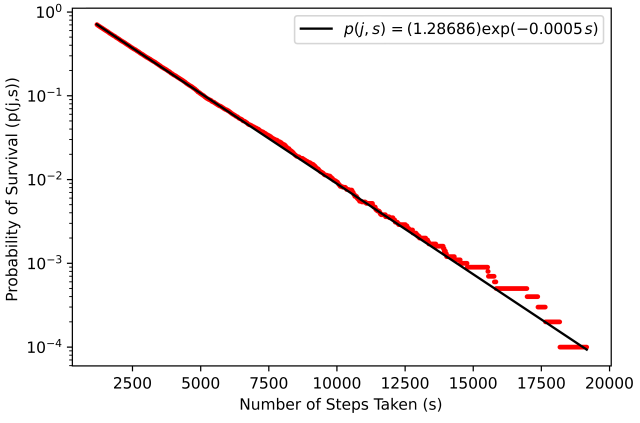

(b) caption

Figure 3: caption

	Ground State		First Excited State	
Well Type	Mean $\lambda J^2 \pm$ SD	Expected	Mean $\lambda J^2 \pm$ SD	Expected
1D	1.205 ± 0.084	1.2337	4.927 ± 0.097	4.9348
2D square	1.213 ± 0.108	1.234	3.017 ± 0.086	3.084
2D circular	1.472 ± 0.085	1.446	7.656 ± 0.074	7.618
	Second Excited State		Third Excited State	
Well Type	Mean $\lambda J^2 \pm$ SD	Expected	Mean $\lambda J^2 \pm$ SD	Expected
1D	11.161 ± 0.061	11.1033	19.711 ± 0.112	19.7392
2D square	4.944 ± 0.114	4.935	6.184 ± 0.071	6.169
2D circular	18.745 ± 0.084	18.722	34.725 ± 0.108	34.760

Table 1: caption

times and taking the mean and standard deviation of the results.

Running the simulations 10 times for 10000 drunkards in wells of $J = 50$ yielded the results shown in Table 1 for the first four energy levels of the 1D infinite potential well, the 2D infinite square well and the 2D infinite circular well. The mean and expected values are quoted up to the first two decimal placements that vary.

5 Conclusions

This work aimed to find good estimates of the energies of the 1D infinite potential well and the 2D infinite square and circular wells using RW simulations

It also looked to investigate how the accuracy of these estimates changes with the well length and the number of drunkards in the simulation, and showed that simulations in larger wells with more drunkards provide better approximations of the ground state energy of the 1D well. This is due to this method relying on the assumption that the probability of the drunkards 'surviving' up to a given number of steps varies smoothly with the drunkard's position and number of steps. A wider well means that the drunkards will be able to take a larger amount of steps before arrest, and more drunkards increases the sample size which creates a smoother probability distribution.

The ground state and first, second and third excited state energies of the 1D, 2D square and 2D circular wells were accurately calculated up to the first decimal placement (Table 1). These estimates could be improved by increasing parameters mentioned above, which would make the simulations more computationally demanding.

In conclusion, while this technique does not provide energy estimates for 1D and 2D wells with great accuracy, this work proved that increasing dimensions does not affect the time complexity of the simulations or quality of the results. RW simulations can thus be an extremely powerful tool for finding approximate solutions to problems at much higher dimensions, for which more accurate methods may deteriorate.

A Random walks - the power of random

A random walk is a random process which describes an object's movement on a given N-dimensional space, starting at a defined point. The simplest way to understand this method is to consider a person standing on a line at an arbitrary starting position $p = 0$. The person is only allowed to take steps along that line and there is equal probability of them stepping in either direction at random. The path taken in 50 steps by four different people is shown in Fig. 4.

Walks like the ones in the figure are *simple symmetric random walks*. One would expect the final position p_f of a walk that carries on to infinity to be the origin of the walk, since each step taken av-

erages to zero as the number of walks increases.

However, it is clear from Fig. 4 that a more common result for finite walks is that the person is some distance away from the starting position after a number of steps. Considering the average of the square of the final position instead, it can be verified that the "root-mean-squared" distance from the origin after N steps is indeed $\sqrt{N}$ on average [6].

Naturally, this simplistic approach is somewhat limited in its applications. In fact, the usefulness of the random walk method comes from its incredible adaptability. It can be easily extended to multiple dimensions by drawing additional random numbers that describe the position in those dimensions without deteriorating. It also allows for the seamless introduction biases in the step direction and length, leading to so called *random walks with drift* [7].

Due to this versatile nature, the random walk method lends itself to applications in a wide array of fields, both academic and industrial, to solve problems of various degrees of complexity.

In academia, random walk algorithms have been used to solve the diffusion equation using spiking neuromorphic hardware [8], or model polymer chains as 'ideal chains', which assumes the polymer to be a random walk and neglects any interactions between the monomers, thus allowing for the derivation of the end-end distance of the chain [9]. Furthermore, biased random walk models are used to describe the behaviour of bacteria and other cells in a chemical gradient [10]. The direction of the bias, towards or away from a certain area, represents the concentration of a chemo-attractant or chemo-repellent substance on that area, respectively [11].

In industry, websites such as Twitter have implemented random walks in their 'who to follow' recommendation services [12]. Image encryption methods which utilise random walk algorithms have also been developed [13]. The algorithm is used to scramble pixels within chunks of a picture, which will in turn undergo permutation effectively encrypting the original image. A random walk hypothesis has also been used to model and forecast shares prices

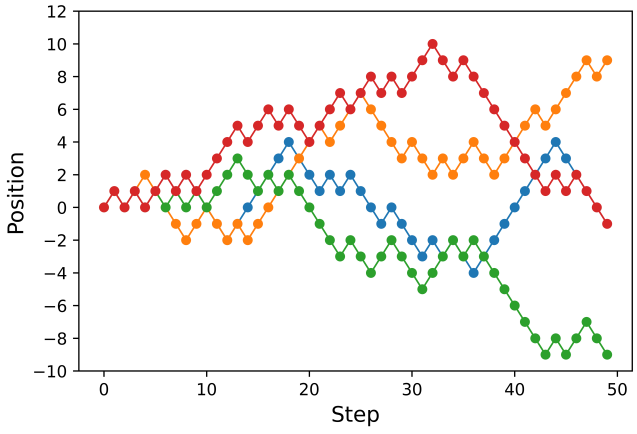

Figure 4: caption

B Python modules

In this project, the direction of each step the walker took was randomly chosen using the `numpy.random` random sampling routine. This routine uses a Permuted Congruential Generator (PCG) as its default pseudo-random number generator (pRNG) [14] which has a period of 2^{128}, a speed of 35.92 Gb/s, and excels at statistical tests, making it an ideal pRNG for the aim of this work [15].

The data fitting was carried out using `scipy.optimise.curve_fit`, which performs non-linear least squares curve fitting using the Levenberg-Marquardt algorithm, an efficient and very robust method of data fitting. The function takes the data to be fitted and the model function as inputs and returns the best-fitting parameters, as well as their covariance matrices. Optionally, it may also take the data uncertainties and initial parameter guesses as inputs, among others [16].

C Derivations

Consider a 2-dimensional lattice upon which a drunkard, whose position is described by x coordinate j_1 and y coordinate j_2, is undergoing a RW. Let us write the probability that the drunkard is at position (j_1, j_2) after s steps as $p(j_1, j_2, n)$ and the probability that the drunkard being arrested at position (j_1, j_2) as $a(j_1, j_2)$. For a drunkard to be at position (j_1, j_2) after $s+1$ steps, they must have been at position $(j_1 \pm 1, j_2)$ or position $(j_1, j_2 \pm 1)$ after s steps. Thus:

$$p(j_1,j_2,s+1) = \frac{1}{2}[1-a(j_1,j_2)][p(j_1-1,j_2,s) + p(j_1+1,j_2,s) + p(j_1,j_2-1,s) + p(j_1,j_2+1,s]$$

If $a(j_1,j_2)$ is very small and s is very large, $p(j_1,j_2,s)$ may be treated as a function of continuous variables j_1, j_2 and s. Using the Taylor series:

$$p(j_1,j_2,s+1) = p(j_1,j_2,s) + \frac{\partial p(j_1,j_2,s)}{\partial s} + ...$$

$$p(j_1-1,j_2,s) = p(j_1,j_2,s) - \frac{\partial p(j_1,j_2,s)}{\partial j_1} + \frac{1}{2}\frac{\partial^2 p(j_1,j_2,s)}{\partial j_1^2} + ...$$

$$p(j_1+1,j_2,s) = p(j_1,j_2,s) + \frac{\partial p(j_1,j_2,s)}{\partial j_1} + \frac{1}{2}\frac{\partial^2 p(j_1,j_2,s)}{\partial j_1^2} + ...$$

$$p(j_1,j_2-1,s) = p(j_1,j_2,s) - \frac{\partial p(j_1,j_2,s)}{\partial j_2} + \frac{1}{2}\frac{\partial^2 p(j_1,j_2,s)}{\partial j_2^2} + ...$$

$$p(j_1,j_2+1,s) = p(j_1,j_2,s) + \frac{\partial p(j_1,j_2,s)}{\partial j_2} + \frac{1}{2}\frac{\partial^2 p(j_1,j_2,s)}{\partial j_2^2} + ...$$

$p(j_1,j_2,s)$ can now be rewritten as a differential equation, neglecting the product of $a(j_1,j_2)$ with second derivative terms as it is very small:

$$\frac{\partial p(j_1,j_2,s)}{\partial s} = \frac{1}{4}\left[\frac{\partial^2 p(j_1,j_2,s)}{\partial j_1^2} + \frac{\partial^2 p(j_1,j_2,s)}{\partial j_2^2}\right] - a(j_1,j_2)p(j_1,j_2,s)$$

Letting $p(j_1,j_2,s)$ take the form $p(j_1,j_2,s) = q(j_1,j_2)\exp(-\lambda s)$, where λ is the rate of arrest and $q(j_1,j_2)$ is an arbitrary spatial distribution, gives an equation of the form of the 2D Schrödinger equation:

$$-\frac{1}{2}\left[\frac{\partial^2 q(j_1,j_2)}{\partial j_1^2} + \frac{\partial^2 q(j_1,j_2)}{\partial j_2^2}\right] + a(j_1,j_2)q(j_1,j_2) = 2\lambda q(j_1,j_2)$$

Now consider the case of a particle in a 2D infinite square well with potential:

$$V(x,y) = \begin{cases} 0 & \text{if } -b < x < band\text{-b<y<b} \\ \infty & \text{otherwise} \end{cases}$$

Let $x = bj_1/J$ and $y = bj_2/J$, so that the Schrödinger equation for this particle can be written in terms of $\psi(j_1,j_2)$:

$$-\frac{\hbar^2}{2m}\left[\frac{J^2}{b^2}\frac{\partial^2\psi(j_1,j_2)}{\partial j_1^2} + \frac{J^2}{b^2}\frac{\partial^2\psi(j_1,j_2)}{\partial j_2^2}\right] + V(j_1,j_2)\psi(j_1,j_2) = E\psi(j_1,j_2)$$

Rearranging this equation and comparing it to the Schrödinger equation of the 2D random walk, assuming $a(j_1,j_2)$ behaves like the potential $V(x,y)$ and both are zero if $|j < J|$):

$$-\frac{1}{2}\left[\frac{\partial^2\psi(j_1,j_2)}{\partial j_1^2} + \frac{\partial^2\psi(j_1,j_2)}{\partial j_2^2}\right] = \frac{mb^2}{J^2\hbar^2}E\psi(j_1,j_2)$$

$$-\frac{1}{2}\left[\frac{\partial^2 q(j_1,j_2)}{\partial j_1^2} + \frac{\partial^2 q(j_1,j_2)}{\partial j_2^2}\right] = 2\lambda q(j_1,j_2)$$

Thus, the energy of a particle inside a 2D infinite square well is:

$$E = \frac{2\lambda J^2\hbar^2}{mb^2}$$

References

[1] J E Neigel and J C Avise. "Application of a random walk model to geographic distributions of animal mitochondrial DNA variation." In: *Genetics* 135.4 (Dec. 1993), pp. 1209–1220. DOI: 10.1093/genetics/135.4.1209.

[2] Eugene F. Fama. "Random Walks in Stock Market Prices". In: *Financial Analysts Journal* 21.5 (Sept. 1965), pp. 55–59. DOI: 10.2469/faj.v21.n5.55.

[3] Tom Weideman. *Infinite Square Well*. Accessed on 16/04/22. URL: https://phys.libretexts.org/@go/page/17172.

[4] Mark E. Tuckerman. *Particle in a 2-Dimensional Box*. Accessed on 16/04/22. URL: https://chem.libretexts.org/@go/page/1725.

[5] Carl W. David. "The Particle in a Box (and in a Circular Box)". In: *Chemistry Education Materials* 12 (June 2006). URL: https://opencommons.uconn.edu/chem_educ/12.

[6] MIT. *Random Walks - The Mathematics in 1 Dimension*. Accessed on 12/04/22. URL: https://www.mit.edu/~kardar/teaching/projects/chemotaxis(AndreaSchmidt)/random.htm.

[7] Fuqua School of Business. *Random walk model*. Accessed on 12/04/22. URL: https://faculty.fuqua.duke.edu/~rnau/Decision411_2007/411rand.htm.

[8] William Severa et al. *Spiking Neural Algorithms for Markov Process Random Walk*. 2018. DOI: 10.48550/ARXIV.1805.00509. URL: https://arxiv.org/abs/1805.00509.

[9] Chinedum Osuji. *Ideal Chain Statistics, Free Energy and Chain Deformation - Hand Out 3 (ENAS 606)*. Jan. 2013.

[10] Wolgang Alt. "Biased random walk models for chemotaxis and related diffusion approximations". In: *Journal of Mathematical Biology* 9.2 (Apr. 1980), pp. 147–177. DOI: 10.1007/bf00275919.

[11] MIT. *Concentration Gradients - And Their Relation to Biased Random Walks*. Accessed on 12/04/22. URL: https://www.mit.edu/~kardar/teaching/projects/chemotaxis(AndreaSchmidt)/gradients.htm.

[12] Pankaj Gupta et al. "WTF: the who to follow service at Twitter". In: *Proceedings of the 22nd international conference on World Wide Web - WWW '13*. ACM Press, 2013. DOI: 10.1145/2488388.2488433. URL: https://doi.org/10.1145/2488388.2488433.

[13] Cong Xu, Jingru Sun, and Chunhua Wang. "An Image Encryption Algorithm Based on Random Walk and Hyperchaotic Systems". In: *International Journal of Bifurcation and Chaos* 30.04 (Mar. 2020), p. 2050060. DOI: 10.1142/s0218127420500601.

[14] NumPy Developers. *Random sampling (numpy.random)*. Accessed on 13/04/22. URL: https://numpy.org/doc/stable/reference/random/index.html.

[15] Melissa E. O'Neill. *PCG: A Family of Simple Fast Space-Efficient Statistically Good Algorithms for Random Number Generation*. Tech. rep. HMC-CS-2014-0905. Claremont, CA: Harvey Mudd College, Sept. 2014. URL: https://www.cs.hmc.edu/tr/hmc-cs-2014-0905.pdf.

[16] The SciPy community. *scipy.optimize.curve_fit*. Accessed on 13/04/22. URL: https://docs.scipy.org/doc/scipy/reference/generated/scipy.optimize.curve_fit.html#scipy.optimize.curve_fit.